



# ***DualProp 4.1 Manual***

# 1. Propeller theories

This chapter describes briefly various analytical propeller theories, which evolved during time. Recently many sophisticated, but computationally expensive, CFD methods were developed. Analytical methods are still useful in for design purposes. Compared to CFD analysis, they lack of flow details, but give good first order predictions in short time.

## 1.1. The Aerial momentum theory of Rankine and Froude

First published work about propellers generating thrust dealt with those used in ships. Pioneer work was done by Mr Rankin and Mr Froude. Mathematical model, which they created described flow through disc and contained many simplifications. Most important simplifications were: incompressibility of fluid, lack of viscosity and assumption that pressure is equal at every point on the disc. Integration of pressure jump in the plane of the disc gave thrust.

## 1.2. The general momentum theory of Betz

One step further included wake swirl behind the disc, which generates additional power losses and it was done by Betz. Calculations accuracy was increased. Momentum theories don't need exact geometry, they base on relations between velocity and momentum in fluid. It simplifies calculations and reduces amount of variables, but still doesn't incorporate some important effects like viscosity.

## 1.3. Blade element theories

Froude who wanted to include more effects, which till that time were omitted formulated blade theory, which was later developed by S. Drzewicki and W.F. Lanchester. This theory needs simple propeller geometry, but it is still assumes 2D flow and doesn't account interference across propeller span. Integrating thrust, moment and drag from propeller blades across span global propeller characteristics are obtained. Such theories don't include flow induction of different parts of propeller and finite length of propeller blades.

## 1.4. Vortex theories

Development of propeller blade theories lead to vortex theories, which account finite length of blades and aerodynamic wake influence on the flow over propeller. Vortex theories allow for design of minimum induced drag propellers. First such theories were formulated by Betz, Glauert and Prandtl, who assumed infinite number of propeller blades and constant distribution of aerodynamic load across span. Wake is considered stiff and has form of a cylinder.

Goldstein was able to account finite number of blades including periodic nature of wake. Wake is represented by helical surface. Vortices are generated on the trailing edge of blades and can have different strength across span. Goldstein introduced new value, circulation of single propeller blade  $K$ , which enables correction for finite number of blades.

Every described theory assumed lightly loaded propeller, where aerodynamic wake stays regular. Theodorsen, who heavily based on Goldsteina work proved, that it is possible to get optimal circulation also on heavily loaded propellers. Transforming heavily loaded propeller case on infinite number of lightly loaded propellers placed one after

another. It is assumed then that wake has helical form in infinity. Theodorsen introduced new values, velocity increased behind propeller referred to undisturbed velocity is marked

$w$ . It's undependable parameter on which every other parameters depend. Also new amended coefficients of mass  $k$  and losses  $\varepsilon$  are tightly coupled with  $w$ .

### **1.5. Analytical model limitations**

None of the presented theories include propeller work on different angle of attack than 0 and interference with airplane components. Boundary layer is treated as quasi 2D. Moreover the program is capable only for one point design, because every time flow parameters are changed optimum load for current conditions is generated. That is why it is not capable of calculating propeller performance for off design conditions.

## 2. DualProp theory

### 2.1. Nomenclature

All used quantities are in SI units. List below shows variables signatures, unit and description of variables.

$L$	[N]	airplane lift force
$B$	[-]	number of thrusting surfaces in the propeller
$c$	[m]	propeller chords
$c_d$	[-]	propeller airfoil drag coefficient
$c_l$	[-]	propeller airfoil lift coefficient
$C_Z$	[-]	airplane lift coefficient
$C_X$	[-]	airplane drag coefficient
$C_T$	[-]	thrust coefficient
$C_Q$	[-]	torque coefficient
$C_P$	[-]	power coefficient
$D$	[m]	propeller diameter
$dP$	[W]	power difference
$J$	[-]	advance ratio $\left(\frac{V}{nD}\right)$
$Jw$	[-]	advance ratio with induced velocity ( $Jw = J(1+w)$ )
$g$	[m/s <sup>2</sup> ]	acceleration of gravity
$K$	[-]	circulation function
$m$	[kg]	airplane weight
$n$	[rev/s]	propeller RPM
$Q$	[Nm]	propeller torque
$P$	[W]	input power to propeller
$P_c$	[-]	ideal power coefficient
$P_{cT}$	[-]	total power coefficient
$P_{req}$	[Nm]	power required to fly
$r$	[m]	radius of propeller section
$R$	[m]	propeller radius
$Re$	[-]	Reynolds number
$S$	[m <sup>2</sup> ]	aircraft wing area
$T$	[N]	propeller thrust
$T_{req}$	[N]	thrust required to fly
$x$	[-]	relative radius of propeller section ( $r/R$ )
$x_o$	[-]	propeller to spinner diameter ratio
$V$	[m/s]	airspeed of aircraft
$V_x$	[-]	linear velocity of propeller section
$w$	[-]	relative velocity increase ( $w/V$ )
$\alpha$	[deg]	airfoils angle of attack
$\beta$	[deg]	propeller angle of attack
$\varepsilon$	[-]	loses coefficient
$\eta$	[-]	propeller efficiency
$\kappa$	[-]	mass coefficient
$\rho$	[kg/m <sup>3</sup> ]	air density
$\nu$	[m <sup>2</sup> /s]	kinematic viscosity
$\sigma$	[-]	propeller element solidity ( $Bb/2\pi r$ )
$\sigma_{c_l}$	[-]	propeller element load coefficient
$\varphi$	[deg]	angle of resultant velocity $w$ at plane of rotation
$\varphi_o$	[-]	$\left(\varphi_o = \text{atg}\left(\frac{J}{\pi x}\right)\right)$
$t$	[s]	time

Subscripts:

F - front, front blade

R - rear, rear blade

## 2.2. Methodology of propeller design

Computer code for the design of the counter-rotating propeller was developed according to Theodorsen theory published in [10-13]. Usage of computer power helped to enhance calculations, which are conducted iteratively. The procedure works according to the following rules.

Propeller design point is set by airplane's steady flight conditions derived from basic Newton laws, assuming that the lift has to be equal to the weight (1) and that the thrust has to be equal to the drag (2).

$$L = mg = \frac{1}{2} \rho V^2 S C_z \quad (1)$$

$$T_{req} = \frac{1}{2} \rho V^2 S C_x \quad (2)$$

Assuming weight, wing area, air density, and cruise speed is known, it is possible to calculate the design lift coefficient from equation (3).

$$C_z = \frac{2mg}{\rho V^2 S} \quad (3)$$

This allows calculating required thrust and power (4) for steady flight conditions and since direct relation between lift coefficient and drag coefficient is known from wind tunnel tests of the airplane [8].

$$P_{req} = T_{req} V \quad (4)$$

Other design parameters like RPM, propeller diameter and spinner diameter are selected arbitrarily by the designer.

Optimal aerodynamic load distribution  $\sigma c/l$  is calculated according to the paper about practical implementation of Theodorsen theory [14]. Power required to fly is put into the equation defining the total power coefficient of the propeller (5).

$$P_{cT} = \frac{P_{req}}{\frac{1}{2} \rho V^3 \pi R^2} \quad (5)$$

It is approximately equal to the ideal total power coefficient (6).

$$P_{cT} \approx P_c = 2\kappa \bar{w} (1 + \bar{w}) \left( 1 + \frac{\varepsilon}{\kappa} \bar{w} \right) \quad (6)$$

Values of  $\kappa$ ,  $\varepsilon$ , necessary in this equation, are taken from charts from experiment related to  $J_w$  (7), and are implemented as polynomials in the design program. [10] describes Theodorsen's research on the optimal circulation distribution about the propeller blade based on the electrical analogy.

$$J_w = \frac{V}{nD} (1 + \bar{w}) \quad (7)$$

To read values of  $\kappa$ ,  $\varepsilon$ , initially  $w$  is assumed to be equal to zero, that allows to determine  $\kappa$ ,  $\varepsilon$  for certain advance ratios calculated from (7). Mass coefficient  $\kappa'$  is corrected according to (8) taking the spinner diameter into consideration.

$$\kappa' = \kappa - x_o^2 K(x_o) \quad (8)$$

Value of  $K(x_o)$  are taken from [15]. Report [15] allows also to determine  $\varepsilon'$  corresponding to  $\kappa'$ . Equation (6) is then rewritten with introduced values of  $\kappa'$ ,  $\varepsilon'$  and solved iteratively for relative velocity increase  $w$  (9),

$$\varepsilon' \bar{w}^{-3} + (\varepsilon' + \kappa') \bar{w}^{-2} + \kappa' \bar{w} - \frac{P_{eT}}{2} = 0 \quad (9)$$

Procedure from (6) - (9) is repeated iteratively. When advance ratio  $J_w$  is calculated with satisfactory accuracy, optimal circulation values  $K(x)$  [15] are determined for certain propeller sections. All information necessary to calculate sufficient front and rear blades twists as well as the load distribution is now available, equations (10), (11), (12), (13), (14).

$$\varphi = \arctan \left( \frac{J}{\pi} \left( \frac{1 + \frac{1}{2} \bar{w}}{x} \right) \right) \quad (10)$$

$$\tan \varphi_F = \frac{J}{\pi x} \left[ 1 + 0.5 \bar{w} \left( 1 + 0.5 \kappa \tan^2 \varphi \right) \right] \quad (11)$$

$$\tan \varphi_R = \frac{J}{\pi x} \left[ 1 + 0.5 \bar{w} \left( 1 - 0.5 \kappa \tan^2 \varphi \right) \right] \quad (12)$$

$$(\sigma_c)_F = \frac{J}{\pi x} \frac{(1 + \bar{w}) \bar{w} \sin \varphi_o}{1 + 0.25 \kappa \bar{w} \sin^2 \varphi_o} K(x) \quad (13)$$

$$(\sigma_c)_R = \frac{J}{\pi x} \frac{(1 + \bar{w}) \bar{w} \sin \varphi_o}{1 + 0.75 \kappa \bar{w} \sin^2 \varphi_o} K(x) \quad (14)$$

Equations (13) and (14) taken for certain sections of blades and divided by the lift coefficient give the chord distribution for both front and rear blades.

$$c_F = \frac{(\sigma_c)_F 2\pi r}{b c_{lF}} \quad (15)$$

$$c_R = \frac{(\sigma_c)_R 2\pi r}{b c_{lR}} \quad (16)$$

Reynolds number is then calculated according to (17) which allows correcting profile drag coefficient. The program tries to balance drag and required thrust, that is why optimum load and profile lift coefficients may change. After every profile lift coefficient change profile drag should be corrected corresponding to actual local lift coefficient and Reynolds number.

$$\text{Re} = \frac{V_x c}{\nu} \quad (17)$$

$$\text{where: } V_x = V \sqrt{1 + \frac{\pi x}{J}} \quad (18)$$

Propeller efficiency and performance is calculated from [15] for assumed geometry and design parameters. Equations (19) and (20) are used to calculate the derivatives of torque coefficients, whereas equations (21) and (22) are used to calculate the derivatives of thrust coefficients for both front and rear propeller.

$$\left( \frac{dC_Q}{dx} \right)_F = \frac{\pi}{8} J^2 (1 + 0.25 \kappa' \bar{w}_F \sin^2 \varphi_o)^2 (\sigma c_l)_F \frac{\cos \varphi_F}{\sin^2 \varphi_o} (\tan \varphi_F + \tan \gamma_F) x^2 \quad (19)$$

$$\left( \frac{dC_Q}{dx} \right)_R = \frac{\pi}{8} J^2 (1 + 0.75 \kappa' \bar{w}_R \sin^2 \varphi_o)^2 (\sigma c_l)_R \frac{\cos \varphi_F}{\sin^2 \varphi_o} (\tan \varphi_R + \tan \gamma_R) x^2 \quad (20)$$

$$\left( \frac{dC_T}{dx} \right)_F = \frac{2 (1 - \tan(\varphi_F) \tan(\gamma_F))}{x (\tan(\varphi_F) + \tan(\gamma_F))} \left( \frac{dC_Q}{dx} \right)_F \quad (21)$$

$$\left( \frac{dC_T}{dx} \right)_R = \frac{2 (1 - \tan(\varphi_R) \tan(\gamma_R))}{x (\tan(\varphi_R) + \tan(\gamma_R))} \left( \frac{dC_Q}{dx} \right)_R \quad (22)$$

Thrust and moment coefficients are given by equations (23), (24), (25), (26).

$$C_{QF} = \int_{x_o}^{1.0} \left( \frac{dC_Q}{dx} \right)_F dx \quad (23)$$

$$C_{QR} = \int_{x_o}^{1.0} \left( \frac{dC_Q}{dx} \right)_R dx \quad (24)$$

$$C_{TF} = \int_{x_o}^{1.0} \left( \frac{dC_T}{dx} \right)_F dx \quad (25)$$

$$C_{TR} = \int_{x_o}^{1.0} \left( \frac{dC_T}{dx} \right)_R dx \quad (26)$$

Power coefficients are calculated from moment coefficients.

$$C_{PF} = 2\pi C_{QF} \quad (27)$$

$$C_{PR} = 2\pi C_{QR} \quad (28)$$

Efficiency is determined from equation (29).

$$\eta = \frac{J(C_{TF} + C_{TR})}{C_{PF} + C_{PR}} \quad (29)$$

Finally torque, thrust and power absorbed by propeller are equal to:

$$T_F = C_{TF} \rho n^2 D^4 \quad (30)$$

$$T_R = C_{TR} \rho n^2 D^4 \quad (31)$$

$$Q_F = C_{QF} \rho n^2 D^5 \quad (32)$$

$$Q_R = C_{QR} \rho n^2 D^5 \quad (33)$$

$$P_F = C_{PF} \rho n^3 D^5 \quad (34)$$

$$P_R = C_{PR} \rho n^3 D^5 \quad (35)$$

Parameters received from these calculations are then compared with thrust and power required for flight. The difference between them is calculated and added to the assumed power which is again used in equation (5)

$$dP = (P_{req} - \eta (PF + PR)) \quad (36)$$

$$P = P + dP \quad (37)$$

Figure 5 shows the propeller blade geometry received with application of this software code for micro UAV described in the introduction.

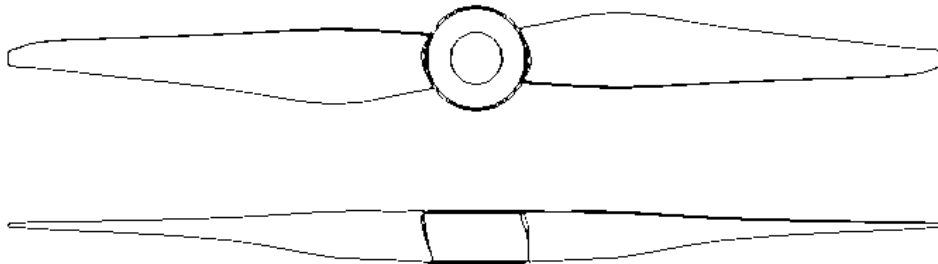


**Fig. 2.1 Blade geometry developed according to Theodorsen theory.**

### 3. DualProp GUI

Program DualProp is based on the methodology described in previous chapter. Fig 3.1 describes geometry definition used in DualProp.

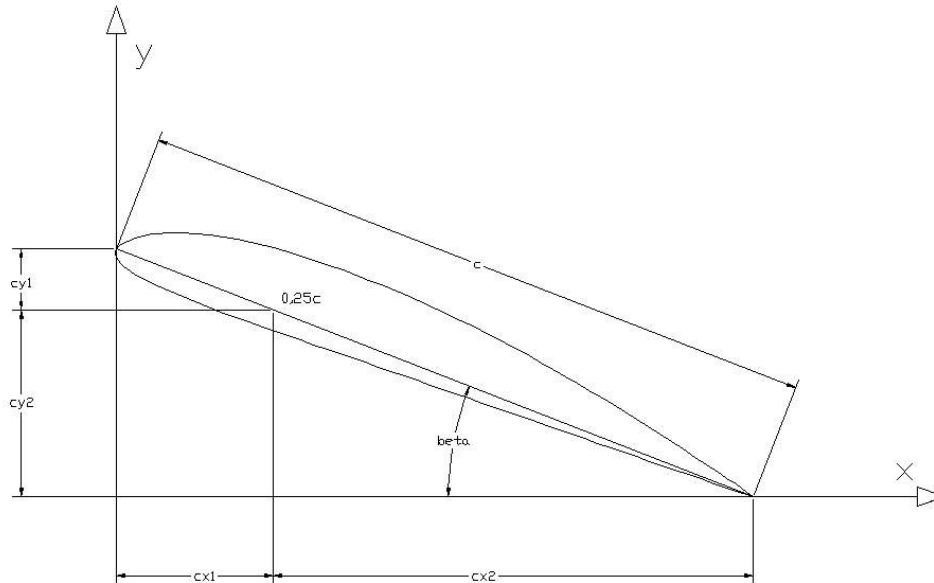


Fig. 3.1 Geometry description in program DualProp.

The program can be started in three different modes:

**1. Interactive:        *DP***

In this mode user simply starts program with GUI, where he can set variables, load or save files and make computations.

**2. With input file:    *DP InputFile***

This modes differs from the previous one only by setting input file during startup.

**3. With output file: *DP InputFile OutputFile***

In this mode program gets input file make computations and writes output results. GUI isn't started at all. It can be very useful if DualProp was used for automated computations as part of computational process, for example for numerical optimization.

File with results contains rewritten input parameters, propeller geometry, propeller characteristics and more. It is easy to recognize parts of the computed data, because signatures in theory are the same.

Fig. 3.2 Presents GUI with *Data* tab visible, after opening the DualProp. On the top of the tab propeller's operation conditions are defined. User specifies required thrust  $T_{req}$ , or power needed to fly  $P_{fly}$ . Next parameters are flight velocity  $V$ , and number of rotations per second  $n$ .  $D_{prop}$  defines maximum diameter of the designed propeller, and  $D_{spin}$  diameter of spinner. Depending on the height of flight,  $\rho$  is air density, and  $\mu$  air viscosity. *Propeller Type* specifies if the propeller is classical one, or counter rotating, and number of blades. If the flag *Set cd Automatically* is checked, angle of attack, and drag on the local airfoil section on the blade is computed, based on the drag model specified in the *Profile Drag* tab. Tables, for front, and rear parts of propeller, specify aerodynamic characteristics of the local airfoil sections on the blades of propeller. First column shows relative position to the total radius of propeller. Next columns are airfoil's angle of attack, lift coefficient, and drag coefficient respectively. The data, also from other tabs, can be read, and saved by the buttons *Read Data*, and *Save Data*. After setting propeller's configuration computations can be done by *Compute* button.

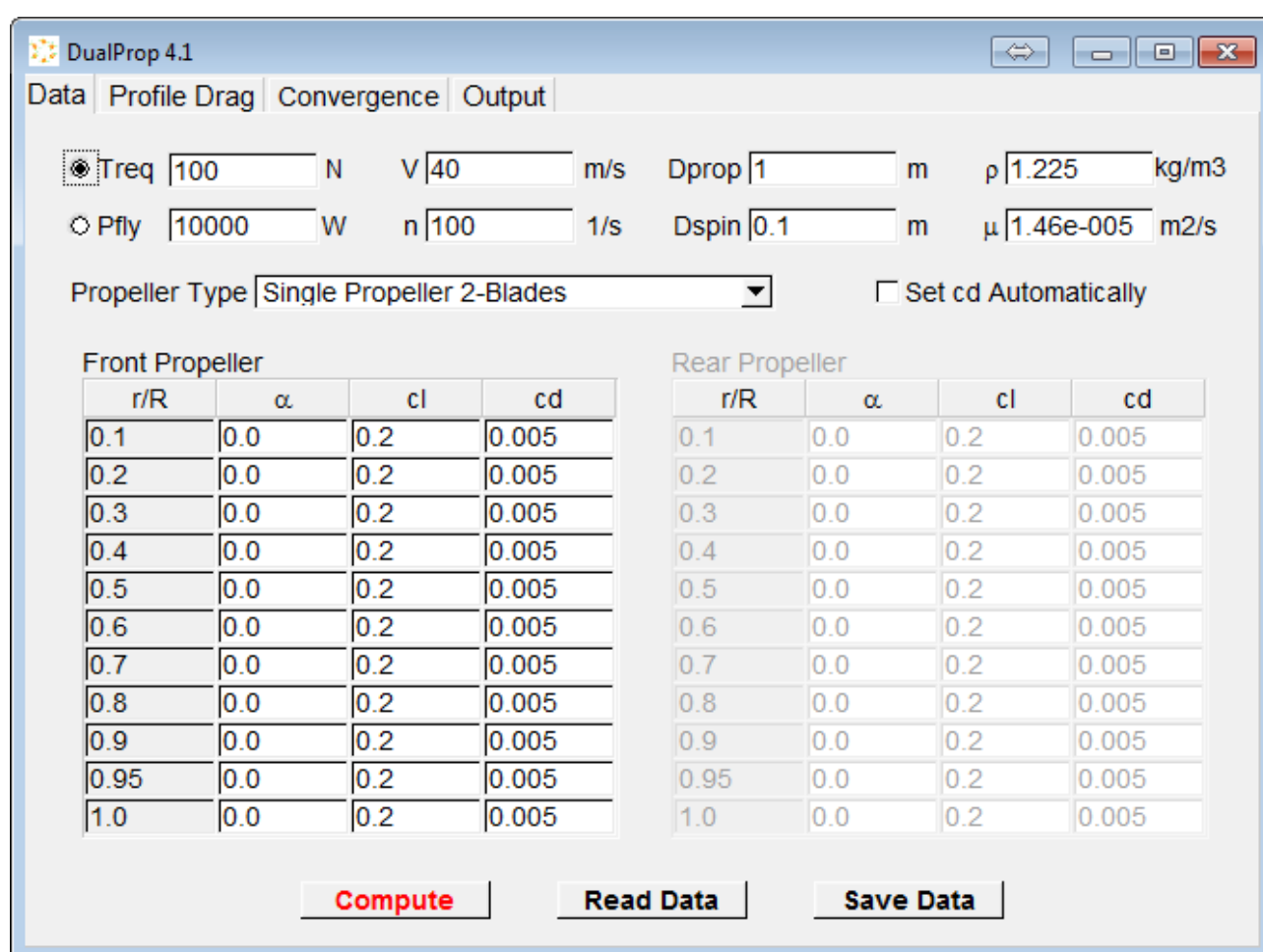


Fig. 3.2 Data tab of the DualProp GUI.

Profile Drag tab Fig. 3.3 specifies two ways how to obtain drag coefficient and angle of attack for local airfoil sections on the propeller's blades, which is set by choosing *cd from*. Analytical model mimics drag polar characteristics of airfoil used, dependent on the Reynolds number, and lift coefficient. The computations are fast, and for the initial design purposes are good enough.

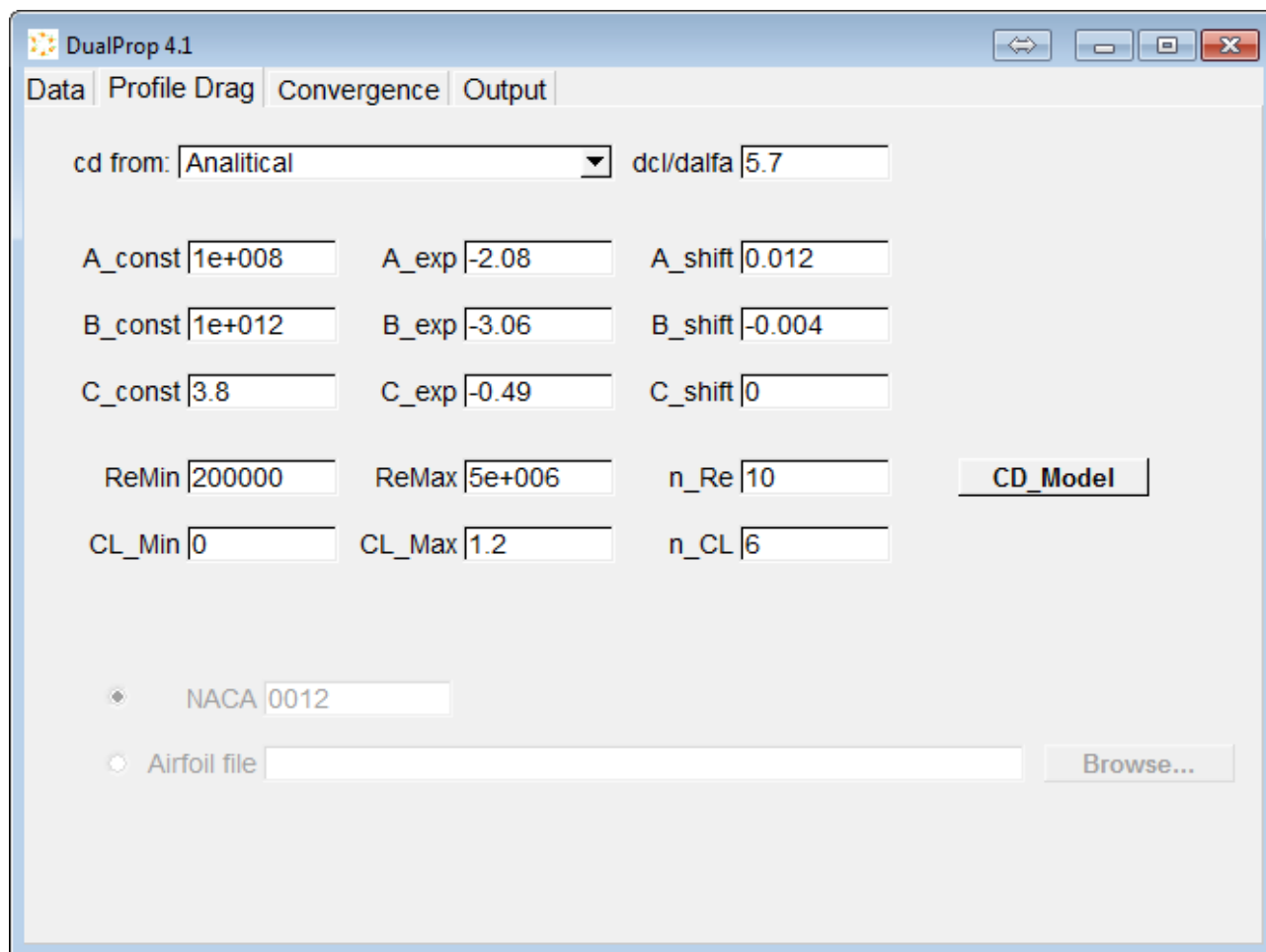


Fig. 3.3 Profile Drag tab of the DualProp GUI – analytical drag model.

Second drag model is based on the coupling of Xfoil program, which utilizes 2D viscous panel method for airfoils analysis. Results are comparable to the experimental data, but multiple airfoil analysis take much more time, than in the case of the analytical model.

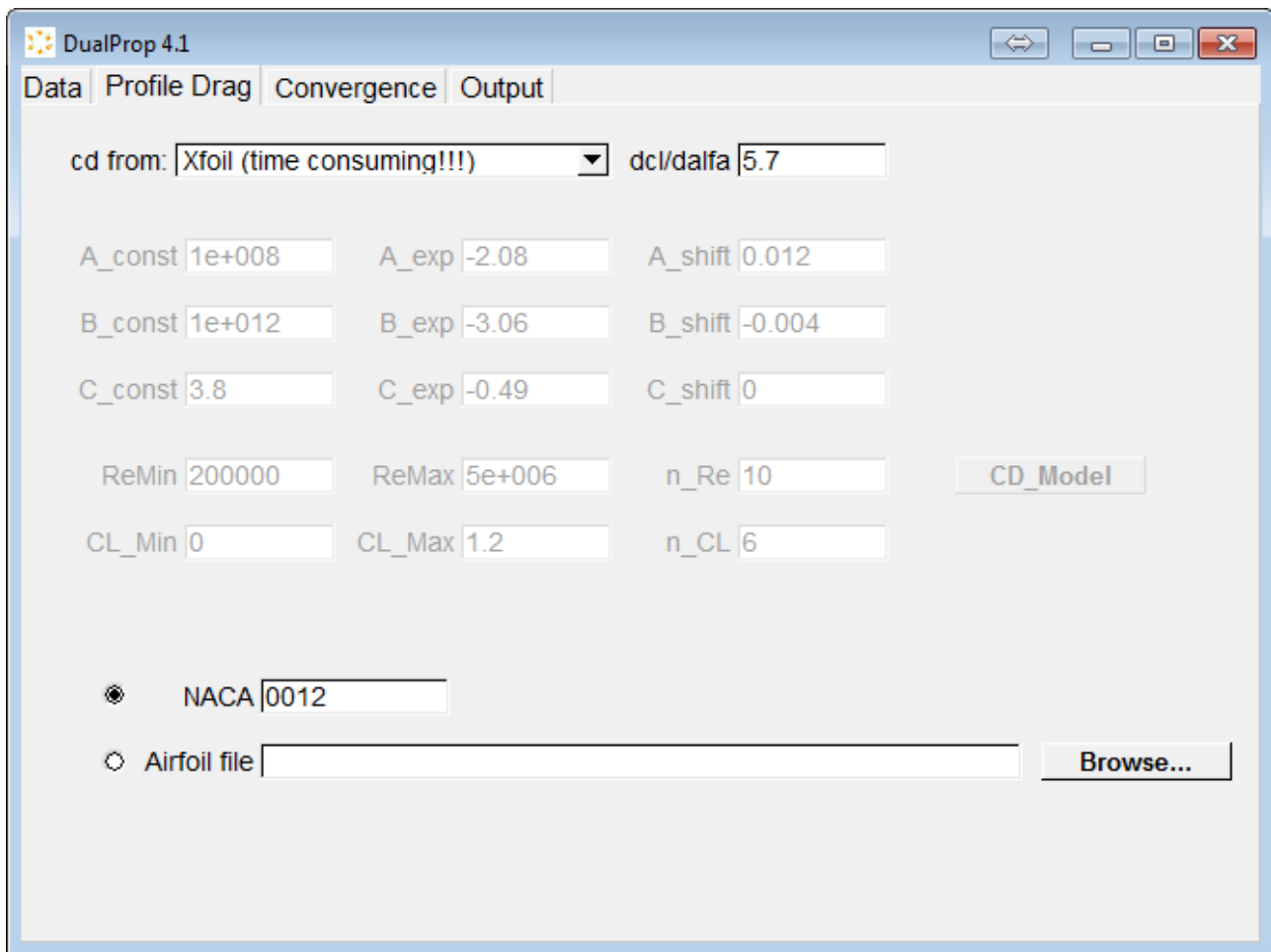


Fig. 3.4 Data tab of the DualProp GUI – Xfoil based drag model.

Convergence tab Fig. 3.5 specifies maximum number of iterations *Max Iter* inside DualProp algorithm loops, which changes time of computations, and accuracy of convergence.  $dw$ ,  $dj$ ,  $dP$  are delta values, which indicate convergence.  $V_{critical}$  defines critical speed at which mach number one is reached.

If the defined configuration is unfeasible warnings may appear, for example when critical speed is reached on the end sections of propeller. Then the configuration has to be changed by propeller's diameter reduction, or rotational speed reduction. Warnings may also appear when the computations didn't converged fully Fig. 3.6. The configuration of the design variables have to be changed. If the inaccuracy, compared to the total value is small, like in the case of power Fig. 3.6, the convergence deltas on the *Convergence* tab can be increased, for example  $dP=1$ .

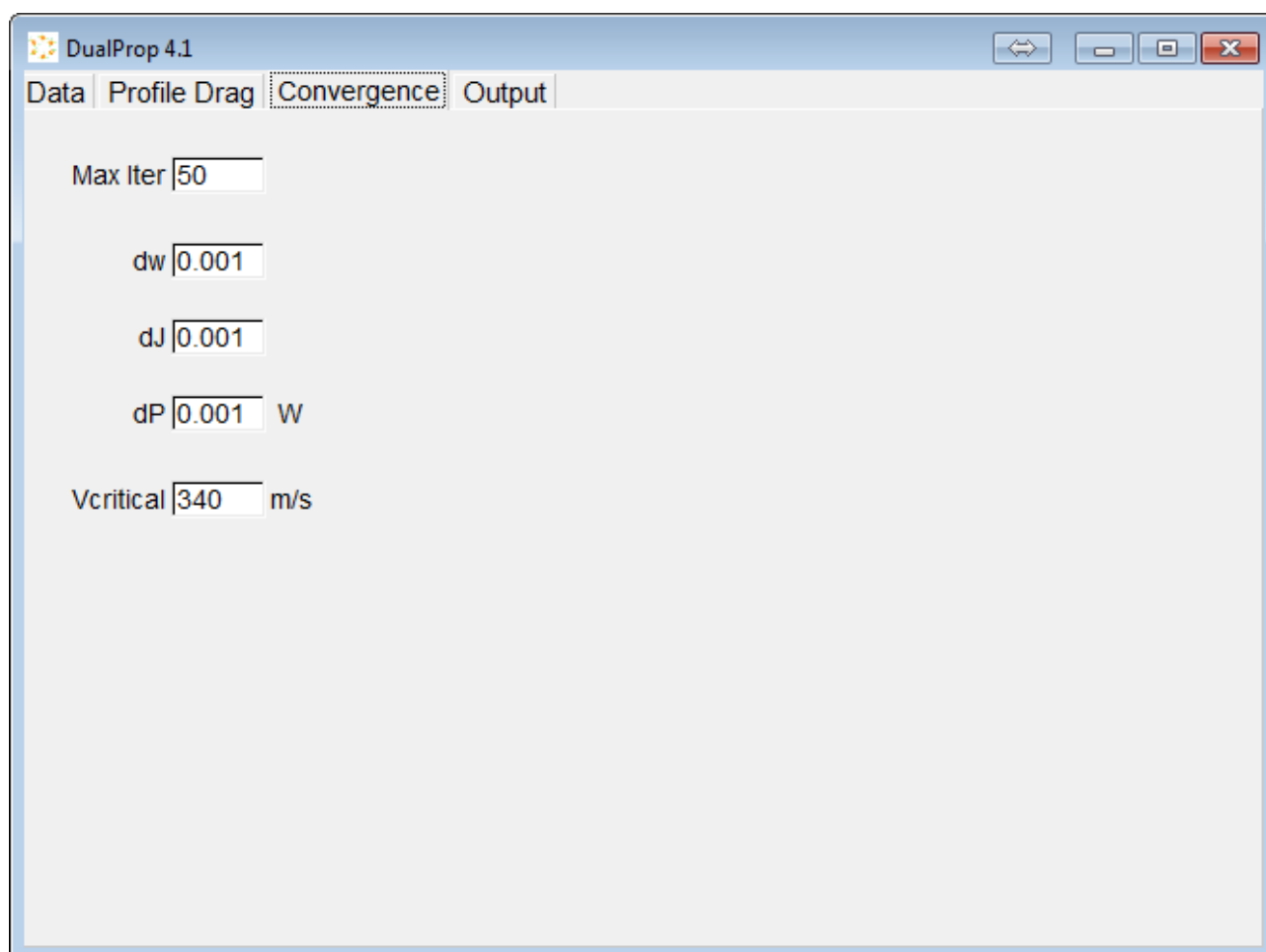


Fig. 3.5 Convergence tab of the DualProp GUI.



Fig. 3.6 DualProp warning message.

*Output* tab Fig. 3.7 presents obtained results, which can be saved by *Save Results* button. After the computations the tab is shown automatically. To turn off the effect, flag *Show Output automatically* has to be unmarked. The propeller can also be investigated visually by pressing button *Visualize* Fig. 3.8.

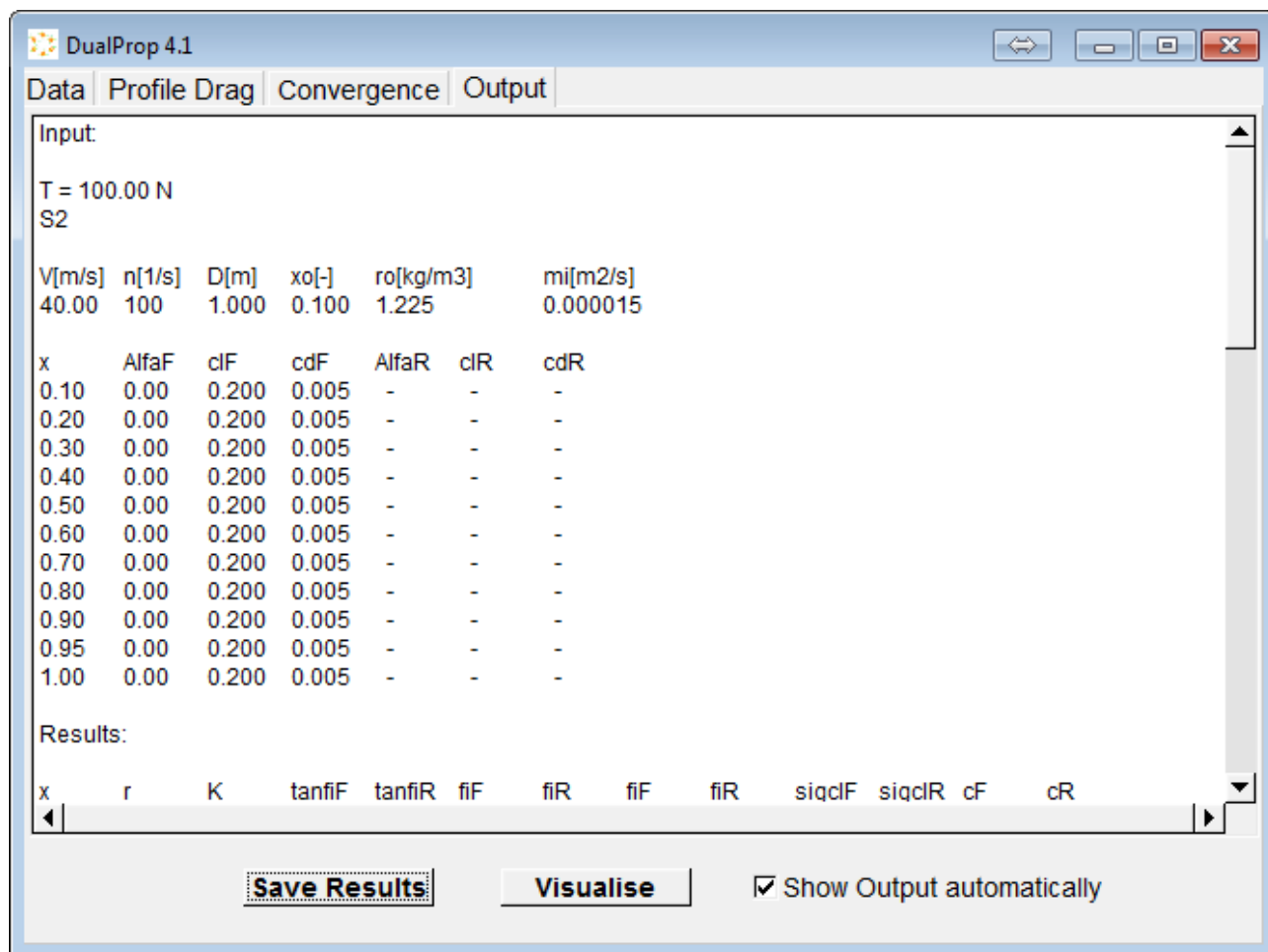


Fig. 3.7 Output tab of the DualProp GUI.

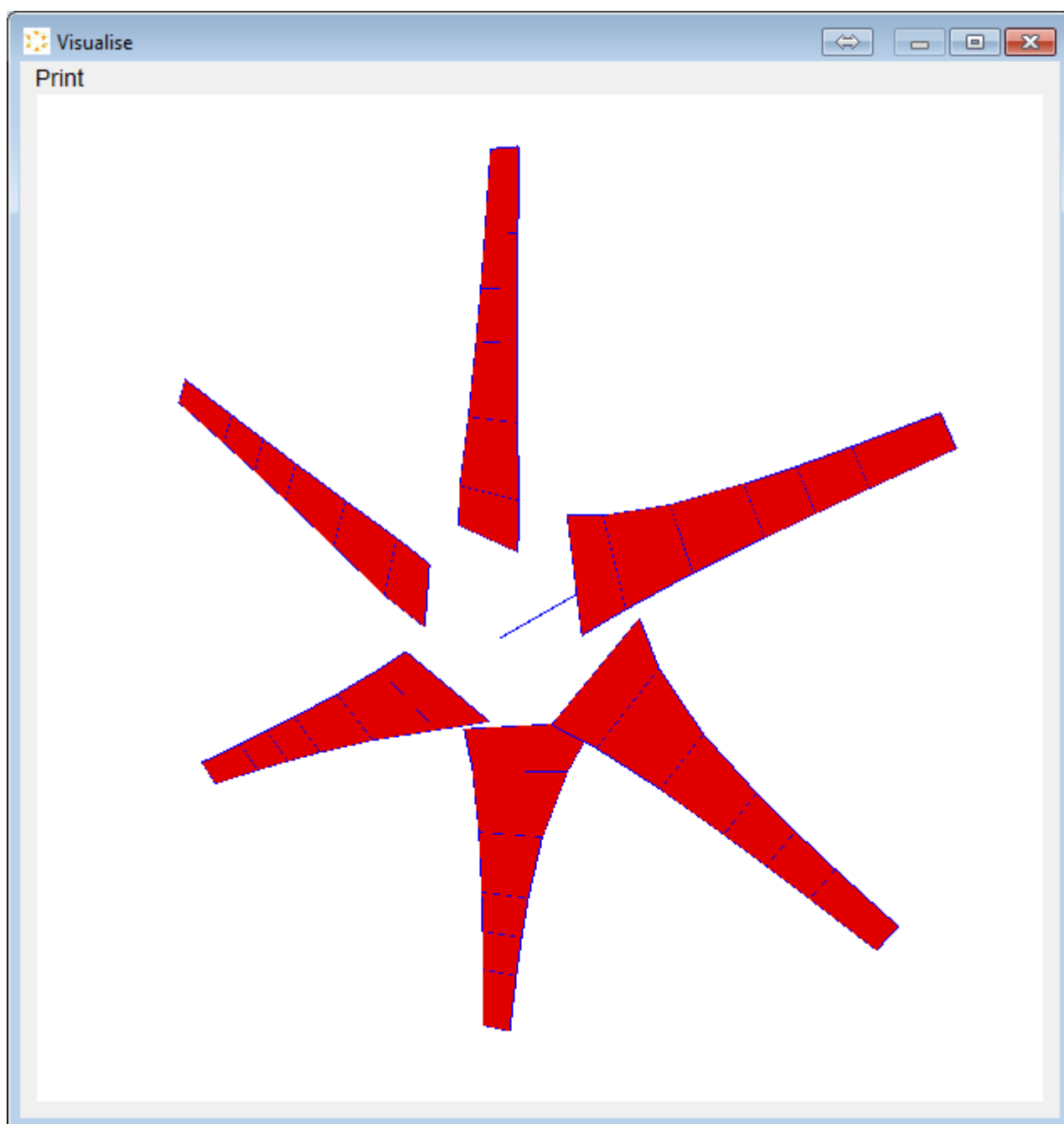


Fig. 3.8 Visualization of a propeller.

## 4. Computations Accuracy

One of the propellers designed in DualProp was tested in a wind tunnel and computed with Fluent software for comparison issues. Charts below Fig. 4.1 – 4.3 show characteristics of thrust, power on a motor’s shaft and propeller efficiency. Quantities on charts are shown from  $J=V/(nD)$ . Blue line shows characteristics of propeller from wind tunnel for the design speed 15m/s in this case. Red points show values obtained from computations in DualProp and Fluent.

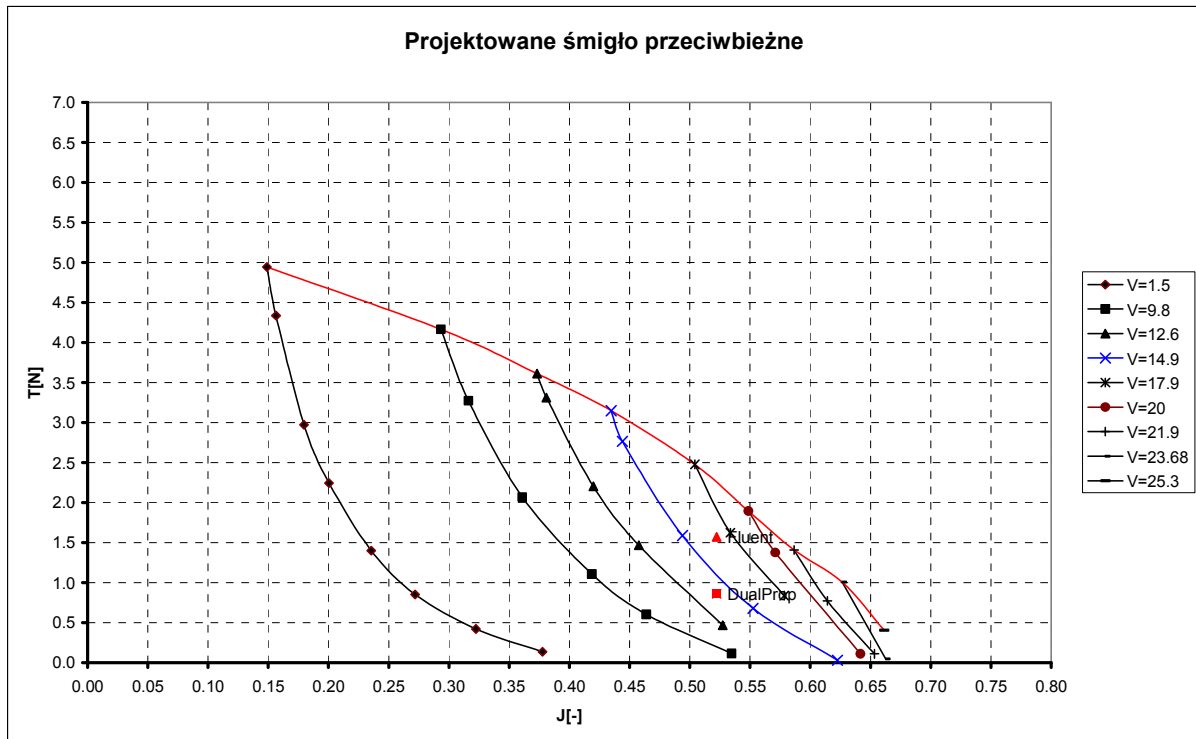


Fig. 4.1 Thrust T from J.

Aerodynamic characteristics of the propeller are very steep and the tested propeller had maximum diameter of only  $D=0.18\text{m}$ . Small changes of propeller work conditions can have big influence on the final characteristics. Although measured inaccuracy of computations to wind tunnel tests is quite big *Tab 4.1*, including disadvantageous circumstances they may be thought as satisfactory. Designing propeller for full size aircraft, will allow for better comparison.

	DualProp	error [%]	Fluent	error [%]	Tunnel
T	0.86	21.9	1.57	42.6	1.1
Pr	40.30	6.1	47.05	23.8	38
ni_śmig	0.32	25.3	0.50	16.3	0.43

Tab 4.1 Error estimation between DualProp computations, Fluent simulation and wind tunnel tests.

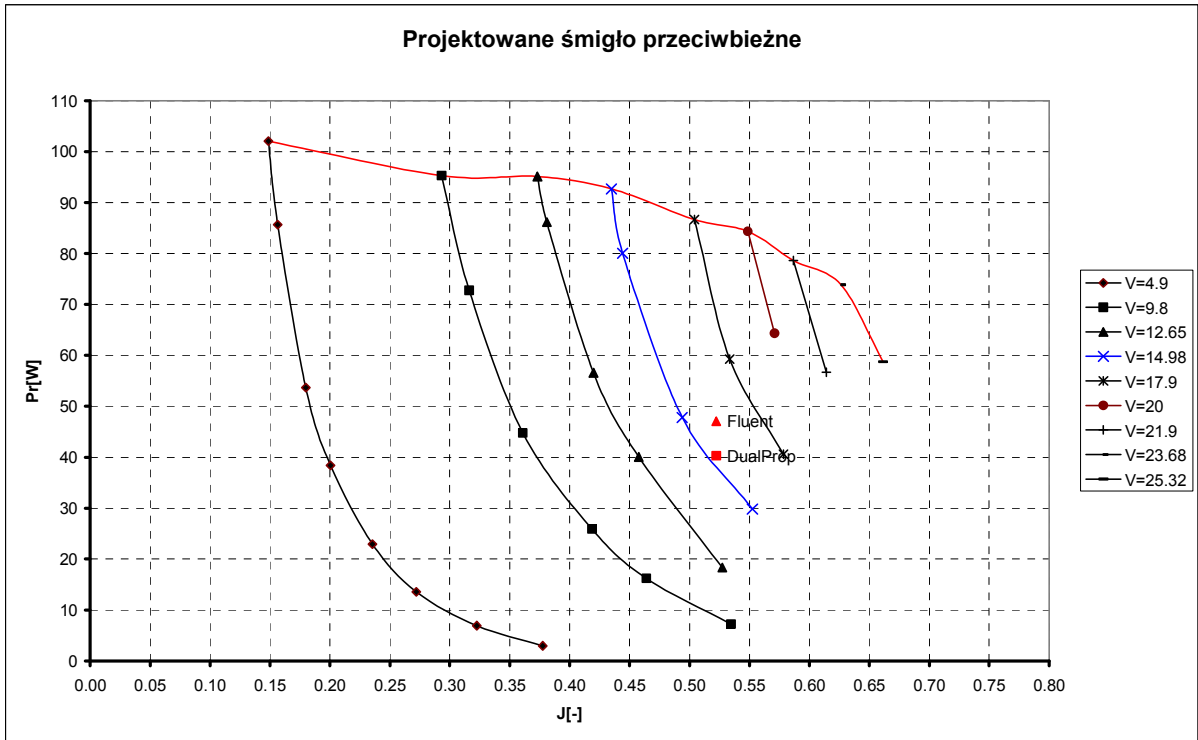


Fig. 4.2 Power on shaft Pr from J.

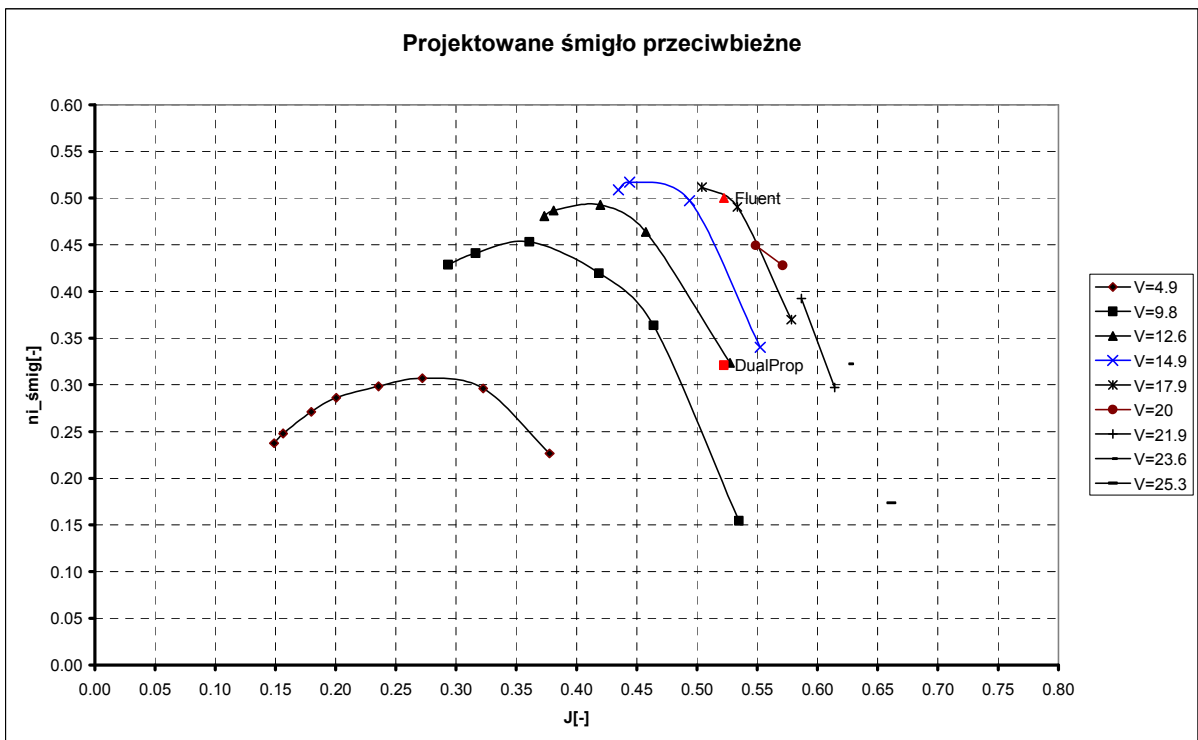


Fig. 4.3 Propeller efficiency from J.



Fig. 4.4 Wind tunnel tests of the designed contra-rotating propeller.